PLANT SCIENCES

Drought will not leave your glass empty: Low risk of hydraulic failure revealed by long-term drought observations in world's top wine regions

Guillaume Charrier,[1,2,3,4]* Sylvain Delzon,[2] Jean-Christophe Domec,[3] Li Zhang,[1]
Chloe E. L. Delmas,[5] Isabelle Merlin,[1] Deborah Corso,[2] Andrew King,[6] Hernan Ojeda,[7] Nathalie Ollat,[1]
Jorge A. Prieto,[8] Thibaut Scholach,[9] Paul Skinner,[10] Cornelis van Leeuwen,[1] Gregory A. Gambetta[1]

Grapevines are crops of global economic importance that will face increasing drought stress because many varieties are described as highly sensitive to hydraulic failure as frequency and intensity of summer drought increase. We developed and used novel approaches to define water stress thresholds for preventing hydraulic failure, which were compared to the drought stress experienced over a decade in two of the world's top wine regions, Napa and Bordeaux. We identified the physiological thresholds for drought-induced mortality in stems and leaves and found small intervarietal differences. Long-term observations in Napa and Bordeaux revealed that grapevines never reach their lethal water-potential thresholds under seasonal droughts, owing to a vulnerability segmentation promoting petiole embolism and leaf mortality. Our findings will aid farmers in reducing water use without risking grapevine hydraulic integrity.

INTRODUCTION

Water availability is one of the most important factors in determining plant survival and productivity in both ecological and agricultural contexts (1). The consumption of freshwater resources for agriculture is enormous, especially in dry environments; for example, 80% of freshwater resources are used for agriculture in California. Thus, reducing crop water use is essential to increase agricultural sustainability. The need to reduce water use, paired with the increased likelihood of large-scale water deficits and extreme drought events (2), is driving the search for more drought-resistant crops. A cornerstone to this pursuit is integrated understanding of the physiological mechanisms driving the resilience of the plant hydraulic system, including water potential (Ψ) and stomatal regulation, vulnerability to embolism along the water column, and ability to recover from drought (3).

One thing is inescapable; as plant water status [that is, leaf water potential (Ψ_{leaf})] declines, plants regulate stomata to control transpirational water loss. Stomatal closure is one of the first responses to drought stress (4), protecting against loss of hydraulic conductivity by maintaining xylem pressure above the onset of embolism (5, 6). Scientists have used a framework to describe variation in stomatal control where a species may be defined as more isohydric or more anisohydric (7–10). Most commonly, iso/anisohydric behavior refers strictly to differences in the regulation of stomatal conductance in response to water deficit,

assuming that stomatal conductance is assessed under identical environmental conditions across decreasing Ψ [for example, see study of Martínez-Vilalta et al. (9)]. But equally, iso/anisohydric behavior can also refer to the regulation of stomatal conductance in response to increasing vapor pressure deficit (D) (11–13). A more isohydric behavior is one where a plant maintains Ψ within a given range under water deficit and high evaporative demand through limiting transpiration. A more anisohydric behavior is one where the plant, to a certain extent, maintains transpiration under water deficit and high evaporative demand, tolerating increasingly negative Ψ. A more isohydric behavior avoids the immediate risk of xylem embolism formation by maintaining Ψ but consequently limits photosynthesis. In the ecological context, interspecific differences in iso/anisohydric behavior between forest trees correspond to differences in their performance and mortality under drought (14). However, this framework is currently debated even at the interspecific level (8–10), and to be of use for the breeding of agricultural crops, differences in iso/anisohydric behavior need to occur at the intraspecific (or intragenus) level.

Grapevines are crops for which different varieties supposedly exhibit contrasting behaviors within the iso/anisohydric paradigm [reviewed by Chaves et al. (15)]. The most classic examples are Grenache (isohydric) and Syrah [anisohydric (16)]. These contrasting varieties are often invoked in a discussion of drought resistance, but it is not entirely clear which would be most beneficial in the context of a woody perennial crop where the iso/anisohydric paradigm constitutes a trade-off between safety with respect to hydraulic failure and productivity. Furthermore, the intraspecific iso/anisohydric behaviors among grapevine varieties can be difficult to separate (17), and individual grapevine varieties can exhibit contradictory behavior depending on the study (15).

Stomatal closure and reductions in transpiration should occur before the onset of embolism (3). Recent work in *Vitis vinifera* suggests that this is indeed the case, where stem embolism occurs at lower (more negative) Ψ [Ψ inducing 50% loss of hydraulic conductivity (Ψ_{50}) < -1.7 MPa] than those typically observed for stomatal closure [Ψ_{leaf} < -1.0 MPa (18)]. The distance between the minimum stem water potential (Ψ_{stem}) experienced in the field (Ψ_{min}) and the Ψ_{50} represents the hydraulic safety margin (19, 20). The smaller this margin,

the more susceptible a plant will be to hydraulic failure. For example, the width of the hydraulic safety margin has been related to differences in drought-induced mortality in trees (21). In perennial crops, the hydraulic safety margin could be important in longevity and long-term productivity under drought. To date, the hydraulic safety margin has not been directly assessed in grapevine, a trait that could potentially differ substantially between varieties exhibiting different strategies for regulation of plant water status.

The current study explores physiological differences in grapevine at the interspecies level by comparing the responses to extreme water deficit (that is, until death of the aboveground biomass) across *V. vinifera* and rootstock varieties. We developed an integrative approach to characterize the dynamic hydraulic strategies of these varieties during increasing drought stress that included the regulation of Ψ_{leaf} (greenhouse versus field plants) and stomatal conductance (at the leaf and whole-plant scale in a greenhouse) in response to a decrease in soil water availability, to plant water status, and to an increase in evaporative demand while accounting for other confounding environmental parameters such as light level. The stem vulnerability to embolism was characterized along the growing season using different techniques [in situ flow centrifuge– and bench-based vulnerability curves, confirmed using high-resolution computed tomography (HRCT)]. For the first time, the safety margin of a range of grapevine varieties was quantified and compared to the in situ water stress experienced in the vineyard across more than a decade in two of the world's most important wine regions.

RESULTS AND DISCUSSION

Unraveling (an-)isohydric behavior by integrating responses to soil water deficit and vapor pressure deficit

Assigning a determined behavior in Ψ regulation is problematic in grapevine (15) and other species (22). *V. vinifera* cv. Grenache and Syrah have repeatedly been described as isohydric and anisohydric, respectively (16, 23). Thus, Grenache would be expected to maintain midday water potential (Ψ_{mdl}) at a higher level than Syrah under similar soil water status [estimated via the relative water content (RWC)] and/or evaporative demand [estimated via the vapor pressure deficit (D)]. Using a large data set of Ψ monitoring across a wide range of drought conditions and combining field observations and greenhouse experiments, we explored the relationship between midday leaf (Ψ_{mdl}) and predawn water potential (Ψ_{pd}). These two varieties did not exhibit significant differences in the relationship between Ψ_{mdl} and Ψ_{pd} (where the slope σ represents the relative sensitivity of the transpiration rate and plant hydraulic conductance to declining water availability) (9), under field conditions (P = 0.074; Fig. 1) nor during a greenhouse drydown experiment (P = 0.225). Additional comparisons also did not reveal significant differences in the relationship between midday stem water potential (Ψ_{mds}) and Ψ_{pd} among three varieties in the Languedoc and two varieties in Saint-Emilion (P > 0.270 and 0.068, respectively; fig. S1). Finally, the water use envelope (24) or "hydroscape" (19) that corresponded to the limit of σ did not exhibit significant differences across varieties (1.32 and 1.38 MPa² for Grenache and Syrah, respectively; Fig. 1).

If (an-)isohydric behavior was genetically determined [for example, see the study of Coupel-Ledru et al. 25], we would expect each variety to exhibit a consistent behavior regardless of the growing conditions. Under field conditions, both varieties exhibited extreme anisohydric behavior (σ = 1.172 ± 0.034 MPa MPa⁻¹, mean ± SE; Fig. 1), whereas
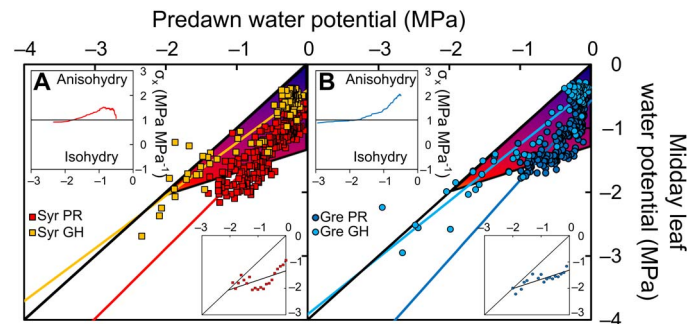
Fig. 1. Ψ_{mdl} depending on Ψ_{pd} in different *V. vinifera* varieties. Syrah (**A**) and Grenache (**B**) were measured in the field [domain "Pech Rouge" (PR); dark colors] and during a drydown experiment in greenhouse (GH; light colors). The slope σ of the linear regressions was not statistically different across varieties in the field (P = 0.074) nor in the greenhouse (P = 0.225). Top left insets represent the slope σ_x (sensitivity to declining water availability) depending on the range of Ψ_{pd} (from 0 to x; x representing the lower limit of the range of Ψ_{pd}) combining field and greenhouse data. Bottom right insets represent the correlation between Ψ_{pd} and minimum Ψ_{mdl} (that is, average value of three lowest Ψ_{mdl} per 0.1-MPa wide class of Ψ_{pd}) combining field and greenhouse data. This linear regression is used to define the lower range of the hydroscape (colored by a blue-to-red gradient representing increasing water stress on the main figure).

partially isohydric behavior was observed in potted plants (σ = 0.861 ± 0.025 MPa MPa⁻¹, mean ± SE; P < 0.001). Synthesizing published studies on these varieties suggests a similar variability between field (16) and potted plants (26).

The ratio between belowground and aboveground biomass was substantially higher in the field than in the greenhouse and likely resulted in differences in accessing soil water. Consequently, the apparent behavior in response to drought may be related to the range of Ψ explored by the plant. Compared to field conditions, greenhouse plants experienced much more negative Ψ_{pd} (−1.4 and −2.9 MPa in the field and greenhouse, respectively). Therefore, we explored changes in σ across an expanding range of Ψ_{pd}:σ_x. The slope σ_x varied widely (top insets in Fig. 1). Under moderate stress ($\Psi_{pd} > -1.5$ MPa), both varieties behaved as extremely anisohydric ($\sigma_x > 1$) and then anisohydric ($\sigma_x = 1$) for $\Psi_{pd} = -1.5$ MPa, whereas they became partially isohydric ($\sigma_x < 1$) under more severe levels of stress ($\Psi_{pd} < -1.5$ MPa). At moderate stress, Syrah exhibits a more pronounced anisohydric behavior according to σ_x, which converges with Grenache as stress levels increase. The current definition regarding the behavior of these varieties may be improved by representing the behavior as dynamic across the (an-)isohydric spectrum, representing an anisohydric to isohydric transition as stress increases.

Neither the dynamics of σ_x (9) nor the hydroscape framework (10) necessitates a linear curve fit. We also explored the framework with nonlinear fits, which improved the statistical significance of the fit [see the estimated Akaike information criterion (AIC); fig. S2], better represented the minimum Ψ, and suggested a slightly larger hydroscape for Syrah (1.42 MPa²) compared to Grenache (1.17 MPa²). This approach also revealed differences between Syrah and Grenache at high Ψ ($\Psi_{pd} > -0.8$ MPa).

Traditionally, the stomatal response to drought stress has been used to assign the (an-)isohydric behavior (7, 14, 16). For instance, anisohydric plants could sustain longer periods of transpiration and photosynthesis under water scarcity, allowing them to be more drought-tolerant than isohydric species (27). If grapevine varieties would regulate Ψ differently,

then it would be observed at the stomatal level as well. However, no significant differences across four contrasting varieties were observed in the decline of stomatal conductance in response to Ψ_{mdl} at the leaf (g_s) or whole-plant (G_s) scale ($P = 0.558$ and 0.164 for g_s and G_s, respectively; Fig. 2, A and B). Equally, no difference was observed in response to Ψ_{pd} ($P = 0.836$; fig. S3). Drawing firm conclusions about differences in leaf-level stomatal conductance (Fig. 2A) is difficult because of the intrinsic variability in the measurement, but this parameter was assessed to complement our whole-plant data (Fig. 2B), which is extremely robust across the full range of Ψ (approximately 5000 data points per variety). These findings are consistent with the lack of differences in leaf intrinsic water-use efficiency reported between isohydric and aniso-hydric genotypes (17).

The transition from anisohydry to isohydry observed here would imply a stronger control of g_s or G_s, especially to D, as drought stress increases. Using a lysimeter platform, we assessed the real-time whole-plant G_s over a 2-month period, exploring the dynamic change in stomatal sensitivity to D during increasing drought stress (fig. S4). To visualize this relationship between G_s and D as a function of plant water status, we used the framework established by Oren et al. (28) in which sensitivity to vapor pressure deficit [that is, dG_s/Ln (D)] is plotted against G_s at 1-kPa vapor pressure deficit (G_{sref}) (Fig. 2C). In all varieties, G_s did not decrease with increasing D until Ψ_{pd} was lower than -0.5 MPa (Fig. 2C, inset, and fig. S4). Dynamic changes in sensitivity revealed that the Ψ threshold at which G_s became sensitivity to D was similar across varieties: $\Psi_{pd} = -0.72 \pm 0.03$ MPa (-0.67, -0.69, -0.71, and -0.80 MPa in Grenache, Syrah, V. riparia, and 110 Richter, respectively). Furthermore, when drought stress increased, the ratio between G_{sref} and sens became constant, reaching the generic value of 0.6 that assumes tight stomatal regulation of Ψ_{leaf} across isohydric species (28).

These dynamics in stomatal regulation with respect to D under decreasing water availability may explain the continuum between anisohydric and isohydric behaviors (8). Well-watered plants exhibited wide variations in σ because Ψ_{mdl} is mainly driven by daily variations in transpiration, and thus, by environmental conditions [that is, light, temperature, and D (29)]. Although plants can exhibit differences under very moderate stress, these differences disappear as water stress increases ($\Psi_{pd} < -0.8$ MPa). These dynamic relationships with respect to soil water and D likely explain the resulting confusion, with respect to either Ψ or stomatal regulation, in assigning a single behavior. Understanding a variety's behavior under drought requires examining stomatal responses with respect to both soil water and D simultaneously across the full range of potential stress levels. Here, we present one possible framework to visualize and quantify soil water deficit/D dynamics in an integrated fashion.

In light of the data presented here, the traditional Grenache/Syrah iso/anisohydric contrast is more nuanced. The relationship between G_{sref} and sens (Fig. 2C) suggests a more anisohydric behavior for Syrah, but these differences are slight and are significant only when particular frameworks are used (that is, Figs. 1 and 2A and fig. S2). In the field, Syrah experiences slightly more negative Ψ than Grenache (Fig. 1 and fig. S2), but at these levels of stress, G_s is nearly zero, suggesting that these differences have to be due to factors other than stomatal regulation per se (for example, differences in cuticular transpiration and/or root hydraulic conductance). Approaches to breeding drought resistance in Vitis based solely on phenotyping differences in stomatal regulation appear insufficient and may benefit from using a more detailed, holistic, and integrative approach like the one used in this study.
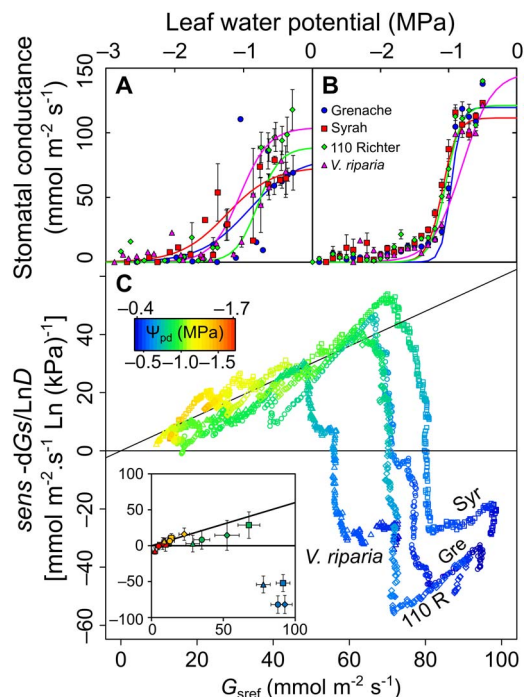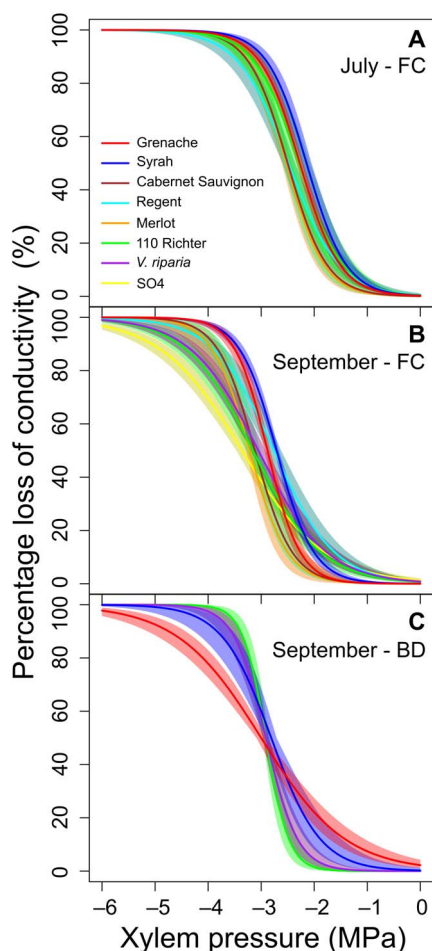

Fig. 2. Response of stomatal conductance depending on decreasing Ψ in different V. vinifera varieties. (**A**) Midmorning (9:00 a.m. to 12:00 p.m.) stomatal conductance measured on individual leaves (g_s), depending on Ψ_{mdl} in four grapevine varieties [V. vinifera cv. Grenache ($n = 58$; blue), V. vinifera cv. Syrah ($n = 61$; red), 110 Richter ($n = 48$; green), and V. riparia ($n = 51$; pink)] during a drydown experiment in greenhouse. (**B**) Midmorning (9:00 a.m. to 12:00 p.m.) stomatal conductance calculated at the whole-plant scale (G_s; obtained from 150 individuals over 2 months) depending on Ψ_{leaf}. Symbol and bars represent the mean and SEs of 0.1-MPa classes. Lines represent the best fit using sigmoid functions for each variety. (**C**) Sensitivity to vapor pressure deficit [that is, dG_s/Ln(D)] depending on G_{sref} in four grapevine varieties (V. vinifera cv. Grenache and Syrah, 110 Richter, and V. riparia), along a water deficit gradient [Ψ_{mdl}, from -0.8 (blue) to -2.3 MPa (red)]. G_{sref} and sensitivity were calculated as the intercept and slope of the logarithmic correlation between G_s and D (as presented in fig. S3) from a sliding frame of 500 consecutive values sorted by increasing drought stress. The line (slope = 0.6) represents the theoretical slope between stomatal conductance at $D = 1$ kPa and stomatal sensitivity to D, which is consistent with the role of stomata in regulating minimum Ψ_{leaf} in isohydric species according to the hydraulic limitation theory (29). The inset represents the estimates (±SE) of G_{sref} and sensitivity at four different level of drought stress: well hydrated (>-0.5 MPa) in blue, mild stress (-0.5; -1.0 MPa) in green, moderate stress (-1.0; -1.5 MPa) in yellow, and severe stress (<-1.5 MPa) in red in four different varieties of grapevine. Syr, Syrah; Gre, Grenache; 110R, 110 Richter.

Stem vulnerability is dynamic, closely following drought intensity along the season

Despite the fact that V. vinifera is adapted to environments experiencing seasonal drought, studies differ in concluding whether it is sensitive (30) or resistant to embolism (31). Because of the similarity in regulating Ψ and stomatal conductance described above, a variety's hydraulic safety margin would ultimately depend on its xylem vulnerability. Therefore, we may expect contrasting varieties to exhibit significant differences in this drought-related trait. Long stems from different varieties were centrifuged to mimic drought stress and induce loss of hydraulic conductivity using the in situ flow centrifuge technique equipped with a 1-m-large rotor. Contrary to all expectations, no significant differences were observed across V. vinifera varieties ($P = 0.67$ and 0.09 in July and September, respectively; Fig. 3, A and B).

These results were confirmed using the bench dehydration method combined with the gravimetric method (Fig. 3C). Different *V. vinifera* varieties consequently exhibit a similar hydraulic vulnerability.

Drought exposure (that is, minimum Ψ_{stem}) is dynamic over the course of the growing season, although no compensatory seasonal changes in stem hydraulic vulnerability have been observed in tree species [32]. Therefore, we could expect the safety margin to be dynamic in relation with the change in drought exposure. Unexpectedly, we found that stem vulnerability was dynamic over the growing season (Ψ_{50} shifted from -2.07 ± 0.08 to -2.82 ± 0.03 MPa in July and September, respectively; Fig. 3). Furthermore, the Ψ_{50} values observed here were lower than those observed at an earlier stage of plant development (May) reported using HRCT [that is, <-1.7 MPa [18]] and were almost identical with the Ψ_{50} values observed in Chardonnay of similar age via nuclear magnetic resonance [31], both noninvasive methods using intact plants. Because plants were continuously well watered from budburst,
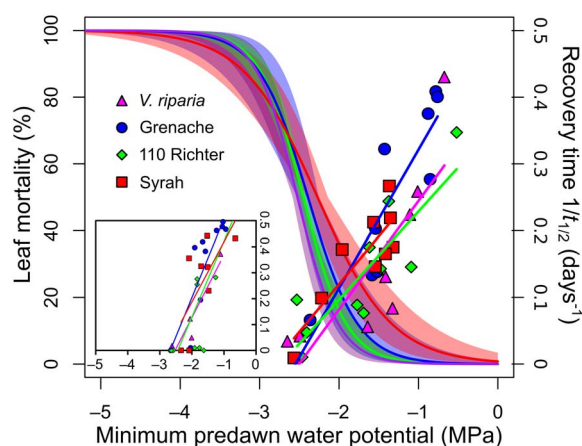
hydraulic conductivity was stable from June to October ($P = 0.387$), and the mean vessel lengths were shorter than 66 cm, changes in hydraulic vulnerability across the season can only be attributed to ontogenic changes. Increased lignification of stem tissues, along with increased thickness of pit membranes from spring to autumn, likely contributes to this increasing resistance to air seeding [33].

Stems originating from rootstocks appeared slightly but significantly more resistant than those of *V. vinifera* [lower Ψ_{50} ($P < 0.001$) and slope ($P < 0.001$; Fig. 3B)]. However, stem vulnerability did not differ across six different grafted combinations between the scions (Grenache or Syrah) and rootstocks [Selection Oppenheim 4 (SO4), *Vitis riparia* 'Gloire de Montpellier' (RGM), or 110 Richter] for Ψ_{50} nor for slope (fig. S5). Previous studies reported changes in drought tolerance conferred by the identity of the rootstock [34]. Because no difference was observed across varieties grafted onto different rootstocks, it is unlikely that these observed differences were brought about by differences in scion stem vulnerability.

Vineyards maintain a significant hydraulic safety margin

Unrecoverable water potential [that is, the Ψ below which transpiration cannot be restored to normal values after rewatering (Ψ_{recov})] varies between plant taxa and has been observed at Ψ_{50} in conifers [3] and at higher losses of conductivity in angiosperms [Ψ_{88} [35] or even Ψ_{99} [36]]. We hypothesized that Ψ_{recov} for grapevine would be similar to other angiosperms. Plants exposed to various levels of drought stress during the greenhouse experiment were rewatered to field capacity, and stomatal conductance was monitored at the leaf and plant scale for several weeks. Surprisingly, stomatal conductance of leaves on rewatered plants did not recover to control levels when Ψ_{pd} reached values lower than Ψ_{50} (that is, Ψ_{recov}; Fig. 4). However, the Ψ_{recov} was similar across varieties [approximately -2.76 ± 0.07 and -2.61 ± 0.08 MPa (that is, approximately Ψ_{50}) at the leaf and whole-plant scale, respectively]. Although some individuals produced new leaves that exhibited normal transpiration, stressed leaves did not recover, most likely because of an increase in leaf abscisic acid concentration [37] and/or petiole and leaf vein embolism. Limited

Fig. 3. Hydraulic vulnerability to drought of different grapevine varieties, seasons, and techniques. (**A** to **C**) Percent stem loss of hydraulic conductivity depending on applied pressure (A and B) or minimum Ψ_{stem} experienced by the plant (C). Vulnerability curves were obtained either during the growing season [$n = 6$ to 8; July (A)] or after growth cessation [$n = 6$ to 8; September (B)], using a dedicated 1-m-diameter Cavitron device. FC, flow centrifuge. Loss of hydraulic conductivity was also measured using the bench dehydration (BD) technique combined with the gravimetric method after relaxation of the tension in the xylem sap [$n = 15$ to 20 (C)]. Lines and colored areas represent modeled vulnerability curves and the confidence interval at 95% for each model.

Fig. 4. Leaf mortality (percent of whole leaves per plant) and recovery time (that is, inverse of the time to recover half of control g_s) versus minimum Ψ_{pd} experienced by different grapevine varieties. The intersection between linear regression and *x* axis gives the minimum Ψ_{recov} for each variety. Lines and colored areas represent modeled leaf mortality curves and the confidence interval at 95% level for each model ($n = 21$ to 24). The inset represents the recovery time measured via G_s (that is, whole-plant stomatal conductance).
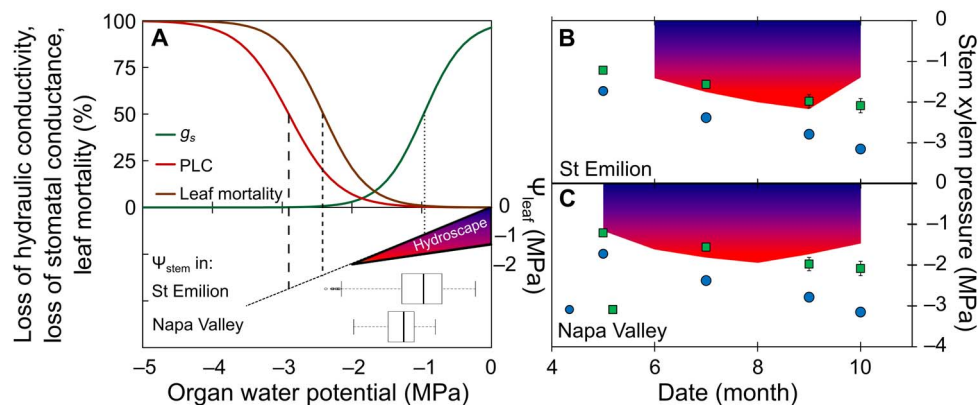
Fig. 5. Physiological thresholds for drought-induced mortality in stems and leaves versus long-term drought survey in Napa Valley and Saint-Emilion. (A) The upper panel depicts stomatal conductance (g_s; green), leaf mortality (brown), and stem loss of hydraulic conductivity (red) depending on organ Ψ. The three curves describe an average *V. vinifera* variety because no significant differences were observed across varieties in the responses of these physiological parameters to Ψ during the greenhouse experiment [namely, Ψ inducing 50% reduction in stomatal conductance (dotted line), leaf vitality (short-dashed line), and stem hydraulic conductivity (long-dashed line)]. The lower panel shows the standardized hydroscape for *V. vinifera* (see Fig.1; colored by a blue-to-red gradient representing increasing water stress), and the box plots depict the distribution of Ψ_{stem} in September observed during a decade in two regions of grapevine production (Saint-Emilion and Napa Valley). PLC, percentage loss of conductance. (**B** and **C**) The observed range of stem xylem pressure (that is, limited by the average of the three minimum Ψ_{stem} observed under field conditions) in Saint-Emilion (B; over the 2003–2016 period in Cabernet Franc and Merlot) and in Napa Valley (C; over the 2010–2016 period in Cabernet Sauvignon, Cabernet Franc, Syrah, and Merlot) per month. In parallel, the dynamic patterns of Ψ_{12} (green squares; mean ± SE) and Ψ_{50} (blue circles; mean ± SE) along the growing season, based on results obtained using HRCT in May (18) and Cavi-1000 (July, September, and October on different *Vitis* varieties—*V. vinifera* cv. Cabernet Sauvignon, Grenache, Merlot, Regent, and Syrah).

transpiration, combined with the hydraulic vulnerability segmentation observed in grapevine petioles, appears to favor leaf shedding under strong and prolonged stress, buffering the perennial organs from reaching lower Ψ (18).

Our greenhouse study demonstrate that when the minimum Ψ leads to 50% loss of stem hydraulic conductivity (that is, Ψ_{50}), the vine sheds essentially all of its leaves (leaf mortality, 83.6%; Fig. 5A). Furthermore, under the most extreme conditions observed over approximately a decade in two major cultivation areas, minimal Ψ_{stem} never reached Ψ_{50} [that is, Saint-Emilion and Napa Valley; Fig. 5], although there was severe leaf drop. These data represent a broad range of field conditions and both nonirrigated (Saint-Emilion and Napa Valley) and irrigated (Napa Valley) vineyards. Midsummer is the period with the smallest hydraulic safety margin, and using the thresholds determined in this study, the most extreme drought events would have only generated an ~25% loss in stem hydraulic conductivity (Fig. 5B). Under the normal operating range of Ψ typically observed in Napa Valley in July (from $\Psi_{pd} = -0.36 \pm 0.01$ MPa to $\Psi_{mds} = -1.15 \pm 0.03$ MPa, mean ± SE), *V. vinifera* cv. Syrah would not present significant level of xylem embolism (Fig. 3A), and this is corroborated in intact plants using HRCT (Fig. 6).

Whereas the extent of drought stress can increase along growing season, so does resistance to embolism. Furthermore, Ψ and g_s regulation prevents Ψ_{stem} from reaching these critical levels, and further protection is proved by petiole embolism and leaf mortality. Although extreme seasons surely result in significant leaf mortality and crop loss, more severe drought-induced embolism appears to be uncommon for grapevine. Nevertheless, the midsummer, with its smaller safety margin, likely represents a critical period when considering management under extreme drought.

CONCLUSIONS

Here, we define the dynamic hydraulic safety margin for grapevine across the growing season and establish Ψ thresholds critical in increasing
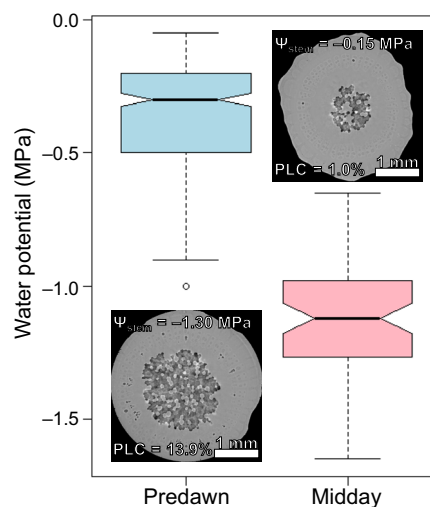
Fig. 6. Distribution of Ψ_{pd} (blue) and Ψ_{mds} (red) water potential observed during June and July in Napa Valley in *V. vinifera* cv. Syrah. The insets represent transverse HRCT images of intact plants from the same variety at Ψ under this normal operating range: from predawn ($\Psi_{pd} = -0.15$ MPa) to midday ($\Psi_{mds} = -1.3$ MPa). Theoretical loss of hydraulic conductivity for each image is calculated from functional (gray) and air-filled (black) xylem vessels and indicated as PLC (%). White bars, 1 mm.

viticultural sustainability and sound water management strategies. Stomatal regulation between supposed contrasting varieties was strikingly similar and dynamic across the (an-)isohydric spectrum, representing an anisohydric to isohydric transition as stress increases. Vulnerability to embolism was almost identical between varieties and was not influenced by rootstock. Nevertheless, it is dynamic across the growing season, decreasing as stress increases. When compared to the drought stress experienced over decades in two of the world's premiere wine regions, severe drought-induced embolism appears to be uncommon for

grapevine. Because of their perennial nature, vineyards are expected to be productive for decades and require a significant up-front investment. Extreme drought can result in vineyards being fallowed; this was the case for tens of thousands of acres during the recent drought in California, with hugely negative economic consequences. The information elucidated here will aid growers in making more intelligent decisions regarding dry farming, fallowing, and irrigation management.

MATERIALS AND METHODS
Greenhouse experiment
Plant material
Dynamic drydown of four varieties of grapevine [V. vinifera cv. Grenache; V. vinifera cv. Syrah; V. rupestris cv. Martin × berlandieri cv. Résséguier no. 2, also known as 110 Richter; and V. riparia cv. Gloire de Montpellier (38)] was measured in a mini-lysimeter greenhouse platform that measures soil water availability and whole-plant transpiration for each individual plant in real time. Temperature, light, and air humidity were monitored every 20 min in two positions of the greenhouse. Air temperature was maintained below approximately 25°C by the greenhouse cooling system, limiting D to approximately 2500 Pa. Cuttings of the year ($n = 33$ per variety), bearing one flushed bud, were planted into 7-liter pots filled with 1 kg of gravel and 5.5 kg of "Terre de Couhins" (20% clay, 18% silt, and 62% sand). Plants were placed in a greenhouse for 2 months before the experiment started and watered with nutritive solution [0.1 mM $NH_4H_2PO_4$, 0.187 mM NH_4NO_3, 0.255 mM KNO_3, 0.025 mM $MgSO_4$, 0.002 mM Fe, and oligo-element (B, Zn, Mn, Cu, and Mo)] to prevent any deficiency during the experiment. Plants were not pruned or damaged during the course of the experiment to avoid air seeding in the xylem. On 16 August 2015, plants were watered to field capacity—watered to saturation at the end of the afternoon and drained overnight. Drought stress was induced on 27 plants per variety by stopping irrigation at three different dates: 26 August on 12 plants per variety, 10 September on 12 plants per variety, and 22 September on 5 plants per variety.

Every 2 to 3 days, Ψ_{pd} was measured on one basal leaf per plant before any light exposure (between 5:00 a.m. and 7:00 a.m.) on three to five plants per variety and treatment. Between 12:00 p.m. and 2:00 p.m., minimum Ψ_{leaf} (Ψ_{mdl}) were measured on the same plants, on fully expanded leaves on which gas exchange was measured (see below). For hydraulic conductivity measurements, Ψ_{mds} values were measured between 12:00 p.m. and 2:00 p.m. on fully expanded leaves, which were bagged in plastic covered with aluminum bags from 7:00 a.m. All Ψ values were measured using a Scholander pressure chamber (Precis 2000).

On every sampled leaf, leaf area and length (using a leaf area meter; WinFOLIA 2007b, Regent Instrument) and dry weight (after oven drying for 1 week at 60°C) were measured (approximately 200 leaves per variety). Dead leaves (visual estimation) were counted on every sampled (hydraulic measurement) or under recovery plant. Total plant leaf area (A_L) was assessed (i) depending on the relation between leaf area and leaf length at the beginning of the experiment (every 2 weeks) and when any change in water regime happened and (ii) depending on the relation between leaf area and leaf dry weight (at the end of the experiment or when a plant was removed from the greenhouse, that is, for hydraulic conductivity measurement). A_L was assumed to change linearly between two measurements, corrected by the area of sampled leaves.

Gas exchange analysis
Leaf gas exchange measurements were conducted between 9:00 a.m. and 12:00 a.m. on mature, well-exposed leaves using a portable open-system including an infrared gas analyzer (GFS 3000, WALZ). Conditions in the cuvette were set steady to conditions that were sub-optimal but easily reproducible all along the experimental period [that is, photosynthetically active radiation (PAR), 1500 μmol m^{-2} s^{-1}; temperature, 20°C, vapor pressure deficit (D), 1 kPa; and CO_2, 400 parts per million).

Balance data analysis
All 132 pots were weighed every 15 min for approximately 2 months on individual scales (CH15R11, OHAUS-type CHAMP). Transpiration per leaf area (E in mol m^{-2} s^{-1}) was estimated as

$$E = \frac{\Delta w}{A_L} \cdot MM_w \qquad (1)$$

where Δw is the change in weight within the considered period (g s^{-1}), A_L is the leaf area (m^2), and MM_w is the molar mass of water (18 g mol^{-1}).

Unrealistic values of transpiration in the data set were filtered out. These values originated from plant watering ($\Delta w > 0$), gas exchange analysis, or other plant manipulations ($\Delta w < -100$ g hour^{-1}). Low A_L (<0.05 m^2) and low Δw (<−2.5 g hour^{-1}; close to balance weight resolution) led to overestimated transpiration rate and were therefore discarded. The whole-plant stomatal conductance G_s (in mol m^{-2} s^{-1} MPa^{-1}) can be calculated as follows (29)

$$G_s = K_G(T) \cdot \frac{k_{tot}}{A_L} \cdot \frac{\Psi_s - \Psi_g}{VPD} \qquad (2)$$

where $K_G(T)$ is the conductance coefficient (in kPa·m^3 kg^{-1}) (39), k_{tot} is the whole-plant hydraulic conductance (in mol s^{-1} MPa^{-1}), Ψ_s and Ψ_g are the Ψ in soil and guard cells, respectively (in megapascals), and D is the vapor pressure deficit (in kilopascals, calculated from temperature and relative humidity data, as indicated in the infrared gas analyzer manual WALZ GFS-3000).

Whole-plant conductance k_{tot} was calculated as

$$k_{tot} = \frac{\Delta w}{\Psi_s - \Psi_g} \cdot MM_w \qquad (3)$$

Finally, using Eqs. 1 to 3, G_s was subsequently calculated as

$$G_s = K_G(T) \cdot \frac{E}{VPD} \qquad (4)$$

On the basis of hourly change in weight (Δw) and relations between RWC, Ψ_{pd}, and Ψ_{leaf}, whole-plant stomatal conductance G_s was compared to leaf level g_s ($R^2 = 0.760$; $P < 0.001$; fig. S6).

Hydraulic conductivity
When targeted Ψ_{mds} values were reached, intact plants were brought to the laboratory for hydraulic conductivity measurements. The main stem was cut under water until a 7-cm-long piece was obtained, originating in the middle of the plant. Each cut was alternately performed at basal and apical end, with a 20-s delay between cuttings to relax sap tension within the xylem and prevent air bubble from expanding at the end of the sample (40). Both ends of the sample were refreshed with a clean razor blade and connected to a tubing system. Flow rate of a degassed KCl (10 mM) and $CaCl_2$ (1 mM) solution was

measured through the sample, from an upper tank to a covered tank placed on a precision electronic balance (0.01-mg resolution; Sartorius). After steady flow was reached (after approximately 30 s to 1 min), mean flow rate was calculated as the average of 10 values measured at 10-s intervals. Flow rate was measured at four different water pressure gradients (ranging from 1 to 3 kPa), according to the procedure described by Torres-Ruiz *et al.* (*41*). Hydraulic conductance of the sample (k_i) was calculated as the slope of the flow rate versus the applied pressure, after verification of the linearity of the relation ($R^2 > 0.99$). Sample was then flushed at high pressure (140 kPa) for 1 min to remove embolism, and conductance was remeasured (k_{max}). PLC was calculated as

$$PLC = \frac{k_{max} - k_i}{k_{max}} \quad (5)$$

Determination of the minimum Ψ_{recov}

The minimum Ψ_{recov} was determined as described by Brodribb and Cochard (*3*). During the recovery phase, the time required for g_s and G_s to reach 50% of its maximum value ($t_{1/2}$) was calculated. Linear regressions were fitted to the inverse of $t_{1/2}$ versus exposed Ψ_{pd}. The Ψ_{recov}, corresponding to the Ψ inducing a failure of g_s and G_s to recover, was assessed by determining the x intercept of the linear regression.

Long-term Ψ field monitoring

Seasonal variations in Ψ_{pd}, Ψ_{mdl}, and Ψ_{mds} water potentials were measured in *V. vinifera* plants growing near Bordeaux [Château Cheval Blanc, Saint-Emilion; Global Positioning System (GPS), 44.92°N, 0.19° W: Saint-Emilion], in California (Napa Valley; GPS, 38.43°N, 122.42° W: Napa Valley) and in Languedoc [Institut National de la Recherche Agronomique (INRA) Pech Rouge experimental unit (Gruissan); GPS, 43.08°N, 3.08°W: Pech Rouge]. In Saint-Emilion, two varieties (Cabernet Franc and Merlot) were monitored over the 2003–2016 period on three blocks with different soil compositions (clay, sand, and gravel). In Napa Valley, three varieties (Cabernet Franc, Cabernet Sauvignon, and Syrah) were monitored over the 2010–2015 period. In Pech Rouge (limestone soil), three varieties (Syrah, Grenache, and Marselan) were monitored in 2005. Ψ values were measured from June until harvest, every 2 weeks (Ψ_{pd} in Saint-Emilion and Pech Rouge and Ψ_{mdl} only in Pech Rouge) or every week (Ψ_{mds} in all locations) according to the procedure detailed below. Ψ_{pd} values were measured on one basal leaf per plant before any light exposure (between 3:00 a.m. and 5:00 a.m.) on 5 to 10 plants per variety and block. Between 1:00 p.m. and 3:00 p.m., Ψ_{mds} values were measured on fully expanded leaves from the same plant, which were bagged in plastic covered with aluminum bags at least 1 hour before measurement. All Ψ values were measured using a Scholander pressure chamber (Saint-Emilion, Precis 2000; Napa Valley, PMS Model-1000; Pech Rouge, Soilmoisture Equipment Corp.)

In situ flow centrifuge technique

Xylem vulnerability to embolism was assessed on different varieties with the Cavitron technique, a centrifugation-based technique, as described by Cochard *et al.* (*42*). Four-year-old plants were not pruned or damaged during the course of the experiment to avoid air seeding in the xylem. Different varieties were used (on $n = 5$ to 6 replicates per variety), either fruit-oriented (*V. vinifera* Syrah, Grenache, Cabernet Sauvignon, Merlot and the interspecific hybrid Regent) or rootstock-oriented (*V. riparia* Gloire de Montpellier, 110 Richter *V. rupestris* ×

berlandieri, and SO4 *V. berlandieri* × *V. riparia*). The basal end of long stems ($L > 3$ m) was cut and shortened to 1-m length under water. The sample was flushed with air at low pressure (1 bar) to empty vessels open on both ends. Centrifugal force was used to establish negative pressure in the xylem and to provoke drought stress–induced embolism, using a custom-built 1-m–diameter honeycomb rotor mounted on a high-speed centrifuge (DG MECA). The xylem pressure, k_i, and PLC were determined at various speeds to obtain a vulnerability curve.

In parallel, maximum and mean vessel lengths were measured by the air injection method. Compressed air was delivered to the basal end of a long stem ($L > 3$ m). Pressure was measured using a manometer and constantly set to 1.8 kPa, whereas air flow was measured using an air flow meter (F111B). The stem was cut shorter until air flowed through the samples (approximately 1 m) and every 10 cm (30- to 100-cm length) and 5 cm (5- to 30-cm length). Air flow was measured at each length after stabilization and computed as indicated by Pan *et al.* (*43*).

High-resolution x-ray computed tomography

Synchrotron-based computed microtomography was used to visualize air- and sap-filled vessels in the main stem of *V. vinifera* cv. Syrah. In spring 2015, six well-watered plants were brought to the HRCT beamline [Pression Structure Imagerie par Contraste à Haute Énergie (PSICHE)] at the Source Optimisée de Lumière d'Energie Intermédiaire du LURE (SOLEIL) synchrotron facility and were scanned immediately and after 6 days of drydown. The Ψ was measured on one leaf, previously wrapped in a plastic bag for 3 hours to provide accurate Ψ_{stem} values with a Scholander pressure chamber (Precis 2000). The middle part of the main stem was scanned using a high-flux (3×10^{11} photons mm^{-2}), 25-keV monochromatic x-ray beam. The projections were recorded with a Hamamatsu ORCA-Flash sCMOS camera equipped with a 250-μm-thick LuAG scintillator. The complete tomographic scan included 1500 projections (50 ms each) for a 180° rotation. Tomographic reconstructions were performed using the PyHST2 software utilizing the Paganin method, resulting in 1536^3 32-bit volumetric images. The final spatial resolution was 3^3 μm^3 per voxel.

The theoretical specific hydraulic conductivity of a whole cross section (K_H) was calculated from the Hagen-Poiseuille equation using the individual diameter of sap- and air-filled vessels as

$$K_H = \sum \frac{\pi \cdot \varnothing^4}{128 \cdot \eta \cdot A_{xyl}} \quad (6)$$

with K_H being the specific theoretical hydraulic conductivity (in kg m^{-1} MPa^{-1} s^{-1}), $\varnothing$ being the mean Feret diameter of vessels (in meters), η being the viscosity of water (1.002 mPa·s at 20°C), and A_{xyl} being the xylem area of the cross section (in square meters).

The theoretical loss of hydraulic conductivity (PLC) was calculated as

$$PLC = 100 \cdot \frac{K_{HA}}{K_{Hmax}} \quad (7)$$

with K_{HA} and K_{Hmax} representing the theoretical hydraulic conductivities of air-filled vessels in initial and cut cross sections, respectively.

Statistical analyses and fit

Statistical analyses and fit were performed using the R software (www.r-project.org). The slope σ of the linear regression between Ψ_{mdl} and Ψ_{pd} was calculated for different varieties and growing conditions (Fig. 1 and fig. S1). For a given variety, the slope σ_x was calculated across different ranges of Ψ_{pd}, that is, from 0 to x MPa (see top inset in Fig. 1 depicting σ in relation with x across the whole range). For each 0.1-MPa Ψ_{pd} class, the average of the three absolute Ψ_{mdl} values was used to calculate the lower limit of the hydroscape, according to the procedure described by Meinzer et al. (10). Accounting for the high variability in Ψ_{mdl} at high Ψ_{pd} (>−0.5 MPa), nonlinear fit was also performed using a composite function

$$\text{For } \Psi_{pd} > \frac{-b}{2 \cdot a} = \Psi_{pd1}; \ \Psi_{md} = a \cdot \Psi_{pd}^2 + b \cdot \Psi_{pd} + c \qquad (8)$$

$$\text{For } \Psi_{pd} < \frac{-b}{2 \cdot a}; \ \Psi_{md} = \min(a \cdot \Psi_{pd1}^2 + b \cdot \Psi_{pd1} + c; \ \Psi_{pd}) \qquad (9)$$

To extrapolate Ψ during the greenhouse experiment, Ψ_{pd} was calculated from RWC through Campbell modified by van Genuchten equation (fig. S7) (44)

$$\Psi_{pd} = a \cdot (\text{RWC})^{-b} + \Psi_e \qquad (10)$$

where Ψ_e is the soil Ψ at the air entry point.

Stomatal conductance, at the leaf (g_s) or plant scale (G_s), depending on Ψ_{mdl}, was fit according to the sigmoid function

$$g_s = \frac{g_{sm}}{1 + e^{slp \cdot (\Psi - g_{s50})}} \qquad (11)$$

where g_{sm} corresponds to maximal stomatal conductance at $\Psi = 0$, slp is the sensitivity to decreasing Ψ, and g_{s50} is the Ψ inducing 50% stomatal closure.

Loss of hydraulic conductivity, depending on minimal Ψ_{stem}, was fit according to the sigmoid function

$$\text{PLC} = \frac{100}{1 + e^{slp \cdot (\Psi - \Psi_{50})}} \qquad (12)$$

where slp corresponds to the sensitivity to decreasing Ψ, and Ψ_{50} is the Ψ inducing 50% loss of conductivity.

Stomatal conductance, at the plant level and under saturating light (PAR > 1500 mmol m^{-2} s^{-1}), was fit in relation with current vapor pressure deficit according to logarithmic function (29)

$$G_s = -m \cdot \text{Ln}(D) + b \qquad (13)$$

where b corresponds to maximal stomatal conductance at $D = 1$ kPa (hereafter called G_{sref}), and m [$-dG_s/d\text{Ln}(D)$] is the sensitivity of G_s to D (sens). For isohydric species, sens was shown to be proportional to 60% of G_{sref} across a wide range of species and varying predictably depending on the range of D used in the analysis (29).

The slope sens and the intercept G_{sref} of the linear regression between G_s and Ln(D) were calculated for each variety and level of water stress (Fig. 2). For a given variety, the slope sens$_x$ and the intercept G_{srefx} were calculated across different ranges of Ψ_{pd}. This method used a sliding window mechanism of G_s/D pair values ranked from 0 to the lowest observed Ψ_{pd} value in which sens$_x$ and G_{srefx} were estimated. The window was divided into a fixed number of equal-sized (500) by step increment of 1 (Fig. 2C).

Across varieties, comparisons in the parameters of different correlations (for example, G_{sref}, sens, and σ_x) were performed using t tests from estimate and SEs as proxy of mean and SEs. Different regressions (that is, linear and nonlinear) of the relation between Ψ_{mdl} and Ψ_{pd} were compared on the basis of the AIC.

REFERENCES AND NOTES

1. C. D. Allen, A. K. Macalady, H. Chenchouni, D. Bachelet, N. McDowell, M. Vennetier, T. Kitzberger, A. Rigling, D. D. Breshears, E. H. Hogg, P. Gonzalez, R. Fensham, Z. Zhang, J. Castro, N. Demidova, J.-H. Lim, G. Allard, S. W. Running, A. Semerci, N. Cobb, A global overview of drought and heat-induced tree mortality reveals emerging climate change risks for forests. For. Ecol. Manage. 259, 660–684 (2010).

2. Intergovernmental Panel on Climate Change, Climate Change 2014—Impacts, Adaptation and Vulnerability: Regional Aspects (Cambridge Univ. Press, 2014)

3. T. J. Brodribb, H. Cochard, Hydraulic failure defines the recovery and point of death in water-stressed conifers. Plant Physiol. 149, 575–584 (2009).

4. T. J. Brodribb, N. M. Holbrook, Stomatal closure during leaf dehydration, correlation with other leaf physiological traits. Plant Physiol. 132, 2166–2173 (2003).

5. M. T. Tyree, J. S. Sperry, Do woody plants operate near the point of catastrophic xylem dysfunction caused by dynamic water stress? Answers from a model. Plant Physiol. 88, 574–580 (1988).

6. H. G. Jones, R. A. Sutherland, Stomatal control of xylem embolism. Plant Cell Environ. 14, 607–612 (1991).

7. F. Tardieu, T. Simonneau, Variability among species of stomatal control under fluctuating soil water status and evaporative demand: Modelling isohydric and anisohydric behaviours. J. Exp. Bot. 49, 419–432 (1998).

8. T. Klein, The variability of stomatal sensitivity to leaf water potential across tree species indicates a continuum between isohydric and anisohydric behaviours. Funct. Ecol. 28, 1313–1320 (2014).

9. J. Martínez-Vilalta, R. Poyatos, D. Aguadé, J. Retana, M. Mencuccini, A new look at water transport regulation in plants. New Phytol. 204, 105–115 (2014).

10. F. C. Meinzer, D. R. Woodruff, D. E. Marias, D. D. Smith, K. A. McCulloh, A. R. Howard, A. L. Magedman, Mapping 'hydroscapes' along the iso-to anisohydric continuum of stomatal regulation of plant water status. Ecol. Lett. 19, 1343–1352 (2016).

11. J.-C. Domec, D. M. Johnson, Does homeostasis or disturbance of homeostasis in minimum leaf water potential explain the isohydric versus anisohydric behavior of Vitis vinifera L. cultivars? Tree Physiol. 32, 245–248 (2012).

12. S. Y. Rogiers, D. H. Greer, J. M. Hatfield, R. J. Hutton, S. J. Clarke, P. A. Hutchinson, A. Somers, Stomatal response of an anisohydric grapevine cultivar to evaporative demand, available soil moisture and abscisic acid. *Tree Physiol.* **32**, 249–261 (2012).

13. Y. Zhang, R. Oren, S. Kang, Spatiotemporal variation of crown-scale stomatal conductance in an arid *Vitis vinifera* L. cv. Merlot vineyard: Direct effects of hydraulic properties and indirect effects of canopy leaf area. *Tree Physiol.* **32**, 262–279 (2012).

14. N. McDowell, W. T. Pockman, C. D. Allen, D. D. Breshears, N. Cobb, T. Kolb, J. Plaut, J. S. Sperry, A. West, D. G. Williams, E. A. Yepez, Mechanisms of plant survival and mortality during drought: Why do some plants survive while others succumb to drought? *New Phytol.* **178**, 719–739 (2008).

15. M. M. Chaves, O. Zarrouk, R. Francisco, J. M. Costa, T. Santos, A. P. Regalado, M. L. Rodrigues, C. M. Lopes, Grapevine under deficit irrigation: Hints from physiological and molecular data. *Ann. Bot.* **105**, 661–676 (2010).

16. H. R. Schultz, Differences in hydraulic architecture account for near-isohydric and anisohydric behaviour of two field-grown *Vitis vinifera* L. cultivars during drought. *Plant Cell Environ.* **26**, 1393–1405 (2003).

17. C. Lovisolo, I. Perrone, A. Carra, A. Ferrandino, J. Flexas, H. Medrano, A. Schubert, Drought-induced changes in development and function of grapevine (*Vitis* spp.) organs and in their hydraulic and non-hydraulic interactions at the whole-plant level: A physiological and molecular update. *Funct. Plant Biol.* **37**, 98–116 (2010).

18. G. Charrier, J. M. Torres-Ruiz, E. Badel, R. Burlett, B. Choat, H. Cochard, C. E. L. Delmas, J.-C. Domec, S. Jansen, A. King, N. Lenoir, N. Martin-StPaul, G. A. Gambetta, S. Delzon, Evidence for hydraulic vulnerability segmentation and lack of xylem refilling under tension. *Plant Physiol.* **172**, 1657–1668 (2016).

19. F. C. Meinzer, D. M. Johnson, B. Lachenbruch, K. A. McCulloh, D. R. Woodruff, Xylem hydraulic safety margins in woody plants: Coordination of stomatal control of xylem tension with hydraulic capacitance. *Funct. Ecol.* **23**, 922–930 (2009).

20. S. Delzon, H. Cochard, Recent advances in tree hydraulics highlight the ecological significance of the hydraulic safety margin. *New Phytol.* **203**, 355–358 (2014).

21. W. R. L. Anderegg, T. Klein, M. Bartlett, L. Sack, A. F. A. Pellegrini, B. Choat, S. Jansen, Meta-analysis reveals that hydraulic traits explain cross-species patterns of drought-induced tree mortality across the globe. *Proc. Natl. Acad. Sci. U.S.A.* **113**, 5024–5029 (2016).

22. J. Martínez-Vilalta, N. Garcia-Forner, Water potential regulation, stomatal behaviour and hydraulic transport under drought: Deconstructing the iso/anisohydric concept. *Plant Cell Environ.* **40**, 962–976 (2017).

23. S. Tombesi, A. Nardini, D. Farinelli, A. Palliotti, Relationships between stomatal behavior, xylem vulnerability to cavitation and leaf water relations in two cultivars of *Vitis vinifera*. *Physiol. Plant.* **152**, 453–464 (2014).

24. J. S. Sperry, U. G. Hacke, R. Oren, J. P. Comstock, Water deficits and hydraulic limits to leaf water supply. *Plant Cell Environ.* **25**, 251–263 (2002).

25. A. Coupel-Ledru, É. Lebon, A. Christophe, A. Doligez, L. Cabrera-Bosquet, P. Péchier, P. Hamard, P. This, T. Simonneau, Genetic variation in a grapevine progeny (*Vitis vinifera* L. cvs Grenache × Syrah) reveals inconsistencies between maintenance of daytime leaf water potential and response of transpiration rate under drought. *J. Exp. Bot.* **65**, 6205–6218 (2014).

26. A. Chouzouri, H. R. Schultz, Hydraulic anatomy, cavitation susceptibility and gas-exchange of several grapevine cultivars of different geographical origin. *Acta Hortic.* **689**, 325–332 (2005).

27. N. G. McDowell, Mechanisms linking drought, hydraulics, carbon metabolism, and vegetation mortality. *Plant Physiol.* **155**, 1051–1059 (2011).

28. R. Oren, J. S. Sperry, G. G. Katul, D. E. Pataki, B. E. Ewers, N. Phillips, K. V. R. Schäfer, Survey and synthesis of intra-and interspecific variation in stomatal sensitivity to vapour pressure deficit. *Plant Cell Environ.* **22**, 1515–1526 (1999).

29. G. Damour, T. Simonneau, H. Cochard, L. Urban, An overview of models of stomatal conductance at the leaf level. *Plant Cell Environ.* **33**, 1419–1438 (2010).

30. A. L. Jacobsen, R. B. Pratt No evidence for an open vessel effect in centrifuge-based vulnerability curves of a long-vesselled liana (*Vitis vinifera*). *New Phytol.* **194**, 982–990 (2012).

31. B. Choat, W. M. Drayton, C. Brodersen, M. A. Matthews, K. A. Shackel, H. Wada, A. J. McElrone, Measurement of vulnerability to water stress-induced cavitation in grapevine: A comparison of four techniques applied to a long-vesseled species. *Plant Cell Environ.* **33**, 1502–1512 (2010).

32. K. Charra-Vaskou, G. Charrier, R. Wortemann, B. Beikircher, H. Cochard, T. Ameglio, T. Mayr, Drought and frost resistance of trees: A comparison of four species at different sites and altitudes. *Ann. For. Sci.* **69**, 325–333 (2012).

33. F. Lens, J. S. Sperry, M. A. Christman, B. Choat, D. Rabaey, S. Jansen, Testing hypotheses that link wood anatomy to cavitation resistance and hydraulic conductivity in the genus *Acer*. *New Phytol.* **190**, 709–723 (2011).

34. I. Serra, A. Strever, P. A. Myburgh, A. Deloire, Review: The interaction between rootstocks and cultivars (*Vitis vinifera* L.) to enhance drought tolerance in grapevine. *Aust. J. Grape Wine Res.* **20**, 1–14 (2014).

35. M. Urli, A. J. Porté, H. Cochard, Y. Guengant, R. Burlett, S. Delzon, Xylem embolism threshold for catastrophic hydraulic failure in angiosperm trees. *Tree Physiol.* **33**, 672–683 (2013).

36. S. Li, M. Feifel, Z. Karimi, B. Schuldt, B. Choat, S. Jansen, Leaf gas exchange performance and the lethal water potential of five European species during drought. *Tree Physiol.* **36**, 179–192 (2016).

37. S. Tombesi, A. Nardini, M. Frioni, M. Soccolini, C. Zadra, D. Farinelli, S. Poni, A. Palliotti, Stomatal closure is induced by hydraulic signals and maintained by ABA in drought-stressed grapevine. *Sci. Rep.* **5**, 12449 (2015).

38. A. Carbonneau, The early selection of grapevine rootstocks for resistance to drought conditions. *Am. J. Enol. Vitic.* **36**, 195–198 (1985).

39. B. E. Ewers, R. Oren, N. Phillips, M. Strömgren, S. Linder, Mean canopy stomatal conductance responses to water and nutrient availabilities in *Picea abies* and *Pinus taeda*. *Tree Physiol.* **21**, 841–850 (2001).

40. J. K. Wheeler, B. A. Huggett, A. N. Tofte, F. E. Rockwell, N. M. Holbrook, Cutting xylem under tension or supersaturated with gas can generate PLC and the appearance of rapid recovery from embolism. *Plant Cell Environ.* **36**, 1938–1949 (2013).

41. J. M. Torres-Ruiz, J. S. Sperry, J. E. Fernández, Improving xylem hydraulic conductivity measurements by correcting the error caused by passive water uptake. *Physiol. Plant.* **146**, 129–135 (2012).

42. H. Cochard, G. Damour, C. Bodet, I. Tharwat, M. Poirier, T. Améglio, Evaluation of a new centrifuge technique for rapid generation of xylem vulnerability curves. *Physiol. Plant.* **124**, 410–418 (2005).

43. R. Pan, J. Geng, J. Cai, M. T. Tyree, A comparison of two methods for measuring vessel length in woody plants. *Plant Cell Environ.* **38**, 2519–2526 (2015).

44. M. T. van Genuchten, A closed-form equation for predicting the hydraulic conductivity of unsaturated soils. *Soil Sci. Soc. Am. J.* **44**, 892–898 (1980).

Citation: G. Charrier, S. Delzon, J.-C. Domec, L. Zhang, C. E. L. Delmas, I. Merlin, D. Corso, A. King, H. Ojeda, N. Ollat, J. A. Prieto, T. Scholach, P. Skinner, C. van Leeuwen, G. A. Gambetta, Drought will not leave your glass empty: Low risk of hydraulic failure revealed by long-term drought observations in world's top wine regions. *Sci. Adv.* **4**, eaao6969 (2018).

ScienceAdvances

Drought will not leave your glass empty: Low risk of hydraulic failure revealed by long-term drought observations in world's top wine regions

Guillaume Charrier, Sylvain Delzon, Jean-Christophe Domec, Li Zhang, Chloe E. L. Delmas, Isabelle Merlin, Deborah Corso, Andrew King, Hernan Ojeda, Nathalie Ollat, Jorge A. Prieto, Thibaut Scholach, Paul Skinner, Cornelis van Leeuwen and Gregory A. Gambetta

ARTICLE TOOLS	http://advances.sciencemag.org/content/4/1/eaao6969
SUPPLEMENTARY MATERIALS	http://advances.sciencemag.org/content/suppl/2018/01/29/4.1.eaao6969.DC1
REFERENCES	This article cites 43 articles, 7 of which you can access for free http://advances.sciencemag.org/content/4/1/eaao6969#BIBL
PERMISSIONS	http://www.sciencemag.org/help/reprints-and-permissions

Use of this article is subject to the Terms of Service